Arch. Metall. Mater. **70** (2025), 4, 1875-1882

DOI: https://doi.org/10.24425/amm.2025.156274

F. CHELGHAM[1*], F. LOURI[1], S. BOUDJEMA[2], A. CHOUKCHOU-BRAHAM[2], Y. BENKRIMA[3*]

OPTIMIZATION OF CYCLOHEXENE OXIDATION USING FRACTIONAL FACTORIAL DESIGN AND V_2O_5/CeO_2 CATALYSTS

An experimental design methodology was applied to optimize cyclohexene oxidation catalyzed by V_2O_5/CeO_2. The statistical study of the process was achieved through a two-level, 2^{5-1} fractional factorial experimental design with five process parameters. The significant input variables (key factors) that influenced the performance of cyclohexene oxidation are the catalyst mass, percentage active phase (catalyst loading), temperature, molar ratio (Cyclohexene/TBHP), and the reaction time. The effect of the individual parameters andtheir interaction effects on the cyclohexene conversion, as well as the selectivity of cyclohexane epoxide, was determined, and a statistical model of the process was developed.The significant parameters influencing conversion were: mass, temperature-molar ratio and time-mass interaction; the other parameters had no effect. Significant parameters influencing selectivity are: molar ratio, other parameters have no effect. The optimal conditions were obtained for the catalyst weight of 0.1 g, temperature of 74°C, and reaction time of 4 h, with 15% V_2O_5/CeO_2 as the active phase and tertiary-butyl hydroperoxide (TBHP) as oxidant.

Keywords: Fractional factorial design; Cyclohexene oxidation; Optimization; Mixed oxides; Vanadia

1. Introduction

Epoxidation catalysis has always been one of the focuses in the chemical science and will continue to attract extensive research in both academia and industry since the epoxides are versatile chemical intermediates for the synthesis of diverse fine chemicals as well as valuable building blocks for the production of polymers, plasticizers and epoxy resins [1-5]. Traditional common oxidants for the epoxidation production are peracids, NaClO and PhIO, which are usually expensive, toxic, and associated with nonselectivity for the epoxide and generation of environmentally undesirable wastes [6-7]. The recent emphasis on overcoming these deficiencies has led to the use of safer, cheaper and more environmentally benign oxidants accompanied with appropriate catalysts. There into, molecular oxygen, aqueous hydrogen peroxide and tert-butyl hydroperoxide (TBHP) are representative oxidants, which has aroused increasing research interests [1,8]. Compared with O_2, which generally shows low efficiency for activation due to its triplet ground state, the use of peroxides can realize the epoxidation reaction processed in liquid phase, contributing to the ease of operation difficulty due to the reduced number of phases and mass transfer limitations. Especially, TBHP has more stability than hydrogen peroxide, and is more prone to supply oxygen atoms resulting from its longer peroxy O-O bond [9-11]. These features endow TBHP a relatively perfect oxidant for initiating the epoxidation reactions under mild reaction conditions.

Among the epoxidation catalysis family, the epoxidation of cycloohexene is an important route for the production of cyclohexene oxide [12]. Catalytic epoxidation of cyclohexene has been conducted in both homogeneous and heterogeneous systems.

Catalytic epoxidation of cyclohexene in the liquid phase is an important reaction used to produce the epoxide that paves the way for the development of soft and green chemistry processes for the synthesis of adipic acid, the raw material used in the production of nylon 6, 6 and tertiary-butyl hydroperoxide (TBHP) as the oxidizing agent [5]. It is used mainly as a source of oxygen for epoxidation reactions, offers a number of advantages such as mildness, selectivity, low corrosivity, low water content

[1] UNIVERSITÉ KASDI MERBAH, FACULTÉ DES HYDROCARBURES; DÉPARTEMENT DE FORAGE ET MÉCANIQUE DES CHANTIERS PÉTROLIERS, ENERGIES RENOUVELABLES; SCIENCES DE LA TERRE ET DE L'UNIVERS, OUARGLA, ALGÉRIE
[2] UNIVERSITÉ DE TLEMCEN, DÉPARTEMENT DE CHIMIE, LABORATOIRE DE CATALYSE ET SYNTHÈSE EN CHIMIE ORGANIQUE, TLEMCEN, ALGÉRIE
[3] ECOLE NORMALE SUPÉRIEURE DE OUARGLA, 30000 OUARGLA, ALGERIA

* Corresponding author: fchelgham @gmail.com

(30%), and is converted to tertiary-butanol after oxidation of olefins [13]. Most transition metal catalysts are highly sensitive to water, which leaches out the metal sites [13].

Transition metal catalysts are the most widely used in oxidation reactions. Among these metals, vanadium is widely used in catalysis as a metal oxide [13]. Supported vanadium oxides play an important role because of their high activity in oxidation reactions [14], such as the oxidation of olefins. The supports generally used are CeO_2, ZrO_2, TiO_2… [14].

More recently, for the purpose of a fundamental study, supported vanadium oxide catalysts have received a particular interest; they constitute a model for catalytic systems 4 because of their activity in a wide range of applications [15], such as many oxidation reactions [16]. During the last decade, catalyst scientists have unambiguously shown that the activity and selectivity of supported metal oxide catalysts are significantly affected by the properties of the support oxide material 5. It has been observed that the selectivity and activity of these catalysts depend on multiple factors, i.e. the vanadium loading, method of support preparation, oxidation state of vanadia in the support, calcination temperature, nature of the support, its surface acidity, etc [17-18]. Several studies have indicated the extent to which vanadia/support interactions may be influenced by dispersion, surface structures, redox and acid-base properties [19-20], base [21-22] and redox properties [23] can be intentionally monitored.

In fact, using different supports and metal loadings, the surface structure [24-25], number of surface sites number of surface sites, the acid-base [21-22] and redox properties [23] can be intentionally monitored. Consequently, considerable attention has been focusedon the preparation, characterization and evaluation of vanadium oxide catalysts deposited on various single or mixed oxides. Cerium based materials were widely used as oxygen carriers [26-27]. The addition of a low amount of cerium can enhance the oxydo-reduction features of a given catalyst. Generally, the oxidation rate is limited by the oxygen transfer from the metal active sites to the metal/support interface, while ceria is able to enhance this oxygen transfer to efficiently catalyze the reaction. The redox properties of ceria (Ce^{4+}/Ce^{3+}) and the high lability of its lattice oxygen are among the most important factors that contribute to the catalytic reactivity in oxidation reactions [28-29]. The presence of vanadia on ceria affords interesting performances for oxidative dehydrogenation reactions [30-32]. The surface polymeric vanadia species on ceria are more reducible than the isolated ones, according to *in situ* Raman spectroscopy [33].

In this study, we are interested in investigating some of the parameters influencing the cyclohexene oxidation reaction using V_2O_5/CeO_2 as catalyst and TBHP as oxidant, adopting the mathematical method, which is the design of experiment specifically the fractional factorial design. The factors chosen are: catalyst mass, temperature, time, percentage in active phase and cyclohexene/TBHP molar ratio. The responsesstudied are conversion and selectivity ofepoxide.

2. Experimental

2.1. Methodology

In this paper, we report the synthesis of vanadia supported ceria catalyts. The V_2O_5 was supported CeO_2 by impregnation method. The catalysts have been characterized by XRD and surface area measurement (BET method). Their catalytic properties were evaluated for cyclohexene epoxidation using tert-butyl hydroperoxide (TBHP) as oxidant. This reaction is influenced by several factors such as catalyst weight, catalyst loading (% of the active phase), reaction temperature (°C), reaction time (h), etc... The experimental design is a suitable tool to recognize significant variables that affect the process and to determine optimal conditions in several processes with limited experimental runs. The technique of experimental design is largely used in chemical industry. For this reason, the aim of our work is to optimize the conditions of the epoxidation reaction of cyclohexene using V_2O_5 supported CeO_2 as catalyst and TBHP as oxidant following a fractional factorial design looking to get a good conversion (Y_1) with good selectivity (Y_2) in epoxide of cyclohexene.

2.2. Catalyst preparation

X % V_2O_5 catalysts are prepared by impregnation according to the method described in the literature [14]. Ceria (CeO_2, Aldrich 99%) in the form of a white powder was first calcined at 400°C with a rate 5°/min for 4 h in air.

The ceria is impregnated with a solution of precursor salt in nitric acid as follows: In a beaker, 32 mL of nitric acid (HNO_3) is added to 0.46 g of precursor salt (NH_4VO_3) and left to stir for 2 hrs. Next, 1.8 g of carrier (CeO_2) is added to the solution. The mixture was left to stir for 24 h [14]. The mixture is placed in a sand bath at 60°C overnight to evaporate the solvent and obtain a dry powder [14]. The solid obtained was then placed in an oven at 120°C overnight [14]. The solid is calcined at 400°C in air for 4 h at a rate of 5°/min [14].

2.3. Catalyst Characterization

The specific surface areas of the samples were determined by BrunauerEmmett-Teller (BET) method using N_2 adsorption-desorption at 77 K on Quantachrome Instruments (Nova 1000e), and the porosity distribution was obtained from the desorption branch of the isotherm using Barrett-Joyner-Halenda (BJH) analysis. The sample was outgassed at 300°C for 8 h. Powder X-ray diffraction (XRD) data were collected on Rigaku D/max2500 diffractometer with Cu Kα radiation (λ = 1.541874 Å) in the range 2θ = 20°-80° with a step of 0.01° and an acquisition time of 1 s.

2.4. Cyclohexene epoxidation

Catalytic tests for cyclohexene epoxidation are carried out as follows: 3 mL (29 mmol) cyclohexene, 15 mL (38.45 mmol) heptane and 1 mL internal standard (1,2-dimethoxyethane) are introduced into a tricol flask fitted with a cooler, magnetic stirrer and thermocouple. When reflux is observed, the TBHP-Heptane mixture (organic phase) is added (20 ml (60 mmol) of Heptane and 5,5 ml (38,4 mmol) of TBHP).

3. Results and discussion

3.1. Characterization of catalysts

Vanadium oxide supported on ceria is characterized with BET and DRX to correlate physico-chemical characteristics with catalytic performance.

The N_2 adsorption-desorption isotherm of the 10% V_2O_5/CeO_2 sample calcined at 400°C and the BJH pore size distribution are shown in Fig. 1.

All the 5, 10, 15% V_2O_5/CeO_2 materials have the same appearance, showing an isotherm that resembles a type IV characteristic of mesoporous materials with a hysteresis that resembles a type H3 according to the IUPAC classification [34].

From these results, we note that commercial ceria has a specific surface area of 41 m^2/g. The TABLE 1 show that the V_2O_5 impregnation initially leads to a decrease in specific surface area (5%V_2O_5/CeO_2, 22 m^2/g) [13], which may be due to instrument error or degassing time, then increases when the samples are calcined at 400 °Cdue to the elimination of physisorbed water molecules and decomposition of the precursor salt (NH_4VO_3) [35]. It can be deduced that the specific surface area increases with calcination temperature (CeO_2, 100 m^2/g at 500°C) and decreases above 500°C [35].

This increase can also be explained by the dissolution and re-precipitation of ceria in the acid solution of the precursor salt [36], or that isolated vanadium oxide particles contribute to the surface [37].

In addition, the pore volume decreases after impregnation, due to the partial obstruction of the ceria pores by the deposition of vanadium metal particles on the outer surface, making it less accessible to nitrogen adsorption [38].

All samples have approximately the same pore diameter of 31 Å (3.1 nm), confirming the presence of mesopores in the catalyst structure (TABLE 1).

The various diffractograms corresponding to X%V_2O_5/CeO_2 materials with different vanadium contents of 5, 10 and 15% are shown in Fig. 2.

TABLE 1

Textural characteristics of different materials as determined by N_2 adsorption

Materials	Calcination temperature (°C)	BET Area (m^2/g)	Pore Volume (cm^3/g)	Pore diameter (Å)
CeO_2	400	41	0,058	31
5% V_2O_5/CeO_2	400	22	0,030	31
10% V_2O_5/CeO_2	400	45	0,048	31
15% V_2O_5/CeO_2	400	65	0,024	31

TABLE 2

Structural characteristics of different materials as determined by XRD analysis

2 Theta (°)	27,8	32,3	46,7	55,7	58,4	68,8	76,1	78,5
(hkl)	(111)	(200)	(220)	(311)	(222)	(400)	(311)	(420)
d_{hkl} (Å)	1,65	1,44	1,06	0,93	0,90	0,82	0,79	0,78
D (Å)	12	14	15	18	19	29	39	47

The diffractograms of the catalysts in Fig. 2 show peaks at around 2Θ = 27.8°; 32.3°; 46.7°; 55.7°; 58.4°; 68.8°; 76.1° and 78.5° associated with pure ceria and corresponding to Miller indices (111), (200), (220), (311), (222), (400), (311) and (420) respectively, showing that ceria has the face-centered cubic fluorite structure [39].

TABLE 2 gives values for the inter-crystal distance 'dhkl' and an estimate of the average crystal size 'D'.

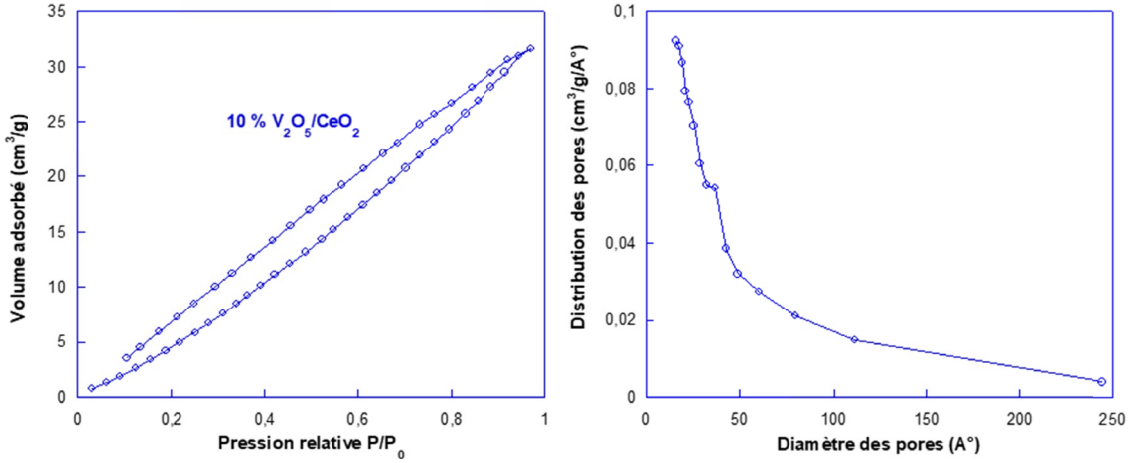

Fig. 1. N_2 adsorption-desorption isotherm for 10% V_2O_5/CeO_2catalysts

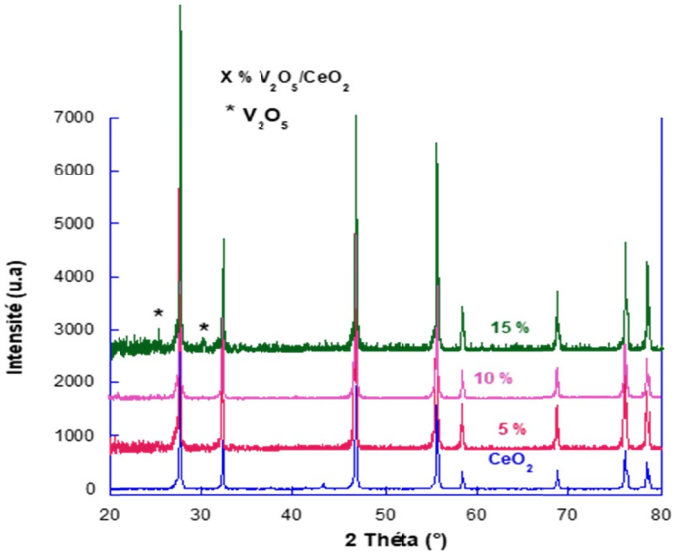

Fig. 2. XRD Diffractograms of CeO_2 and $X\%V_2O_5/CeO_2$

Comparison of the diffraction spectra of ceria and those of the different vanadium percentages indicates that there is no crystalline impurity and that, after impregnation, the diffraction peaks are shifted towards the higher 2Θ and lower interreticular distances. We note that V_2O_5 deposition does not influence the structure of the substrate and remains preserved throughout impregnation, and V_2O_5 peaks are not observed at low contents.

The V_2O_5 crystalline phase is detected at high vanadium contents prepared by impregnation [40], in the case of 15% V_2O_5/CeO_2 low intensity peaks appear at 2Θ = 25.1°, 30.2° indicate the formation of the V_2O_5 crystalline phase [41] .

3.2. Catalytic test

A. Experiment

TABLE 3 shows the two-level experimental matrix (in coded variables) and the results of theexperimental measurements of the responses: conversion of cyclohexene (Y_1), selectivity of cyclohexane epoxide (Y_2) and TBHP consumption. The cyclohexene conversion ranges from 17% to 68%, and the selectivity to cyclohexane epoxide ranges from 35% to 84%, thus indicating the great significance of the chosen parameters of the cyclohexene oxidation.

B. Interpretation of results

Design results are analyzed using Design-Expert software. The influence of the main factors and their interactions is calculated by analysis of variance (ANOVA) with a risk threshold of 5% (α = 0.05; 95% confidence interval) [42].

For the interpretation of a fractional design, the coefficients are aliased in the contrasts and the interpretation assumption 1, which eliminates all interactions of order ≥3 and leaves only interactions of order 2 [43].

TABLE 3

Tests and response of the 2^{5-1} fractional factorial design on catalytic epoxidation of cyclohexene

	Factors					Responses		Conversion of. TBHP (%)
	Percentage in active phase(%)	Temperature (°C)	Time (h)	Molar Ratio	catalyst mass (g)	Conversion (%)	Selectivity of Epoxide (%)	
Run	A	B	C	D	E = ABCD	Y_1	Y_2	
1	–1	–1	–1	–1	+1	38	68	12
2	+1	–1	–1	–1	–1	27	39	15
3	–1	+1	–1	–1	–1	29	68	25
4	+1	+1	–1	–1	+1	56	45	23
5	–1	–1	+1	–1	–1	29	68	31
6	+1	–1	+1	–1	+1	34	58	35
7	–1	+1	+1	–1	+1	30	35	66
8	+1	+1	+1	–1	–1	58	44	58
9	–1	–1	–1	+1	–1	18	75	27
10	+1	–1	–1	+1	+1	48	78	23
11	–1	+1	–1	+1	+1	35	78	42
12	+1	+1	–1	+1	–1	39	78	40
13	–1	–1	+1	+1	+1	37	77	33
14	+1	–1	+1	+1	–1	35	66	30
15	–1	+1	+1	+1	–1	17	73	33
16	+1	+1	+1	+1	+1	22	81	41
17	0	0	0	0	0	48	73	22
18	0	0	0	0	0	50	77	20
19	0	0	0	0	0	68	64	20
20	0	0	0	0	0	54	84	40
21	0	0	0	0	0	63	64	39

C. Mathematical model

We choose the mathematical model with the constant coefficient, the coefficients of the main factors and the 2nd-order interactions.

$$y = a_0 + a_1A + a_2B + a_3C + a_4D + a_5E + a_{12}AB + a_{13}AC + a_{14}AD + a_{15}AE + a_{23}BC + a_{24}BD + a_{25}BE + a_{34}CD + a_{35}CE + a_{45}DE \pm \varepsilon$$

Hence: y is the dependent variable (the two responses) and the factors and their interactions are the independent variables [42].

i. Conversion response

TABLE 4 shows the results of the contrast coefficient calculation. The bar chart in Fig. 3 illustrates this table.

All values below 0.05 (p-value) indicate that the model terms are significant and are: A, BD, CE (the zero does not belong to the confidence domain). The other terms have an effect, but do not reach their threshold values to be significant, and the zero belongs to their confidence domains.

The conversion model equation is therefore as follows:

$$Y_1 = 34{,}63 + 5{,}25A - 4{,}25BD - 5{,}13CE \pm \varepsilon$$

Classification of the coefficients by order ascending:

$$a_A > a_{CE} > a_{BD}$$

ii. Selectivity Response

TABLE 5 shows the results of calculating the contrast coefficients. The bar chart in Fig. 4 illustrates this table.

The equation for the selectivity model is:

$$Y_2 = 64{,}44 + 11{,}31D \pm \varepsilon$$

All values below 0.05 (p-value) indicate that the model terms are significant and are: D (the zero does not belong to the confidence domain). The other terms have an effect, but do

TABLE 4

Coefficient values for the conversion model

Real Factors	Coded Factors	Estimation des coefficients	p-value	Signification	Confidence interval at 95 %	
					Lowerlimit	Upperlimit
Constant	/	34,63	0,03	Significant	30,70	38,55
Percentage in active phase (%)	A	5,25	0,02	Significant	1,32	9,18
Temperature (°C)	B	1,37	0,41	Not Significant	–4,59	7,34
Time(h)	C	–1,87	0,30	Not Significant	–5,80	2,05
Molar ratio	D	–3,00	0,12	Not Significant	–6,93	0,93
Catalyst Mass (g)	E	3,13	0,10	Not Significant	–0,80	7,05
	AB	2,50	0,18	Not Significant	–1,43	6,43
	AC	–0,75	0,12	Not Significant	–6,71	5,21
	AD	–0,88	0,17	Not Significant	–6,84	5,09
	AE	–3,00	0,12	Not Significant	–6,93	0,93
	BC	–2,38	0,20	Not Significant	–6,30	1,55
	BD	**–4,25**	**0,04**	**Significant**	**–8,18**	–0,32
	BE	–2,87	0,13	Not Significant	–6,80	1,05
	CD	–2,00	0,27	Not Significant	–5,93	1,93
	CE	**–5,13**	**0,02**	**Significant**	**–9,05**	**–1,20**
	DE	1,25	0,34	Not Significant	–4,71	7,21

$R^2 = 0.85$ and $R^2_{adj} = 0.63$ means that the conversion model is 85% reliable.

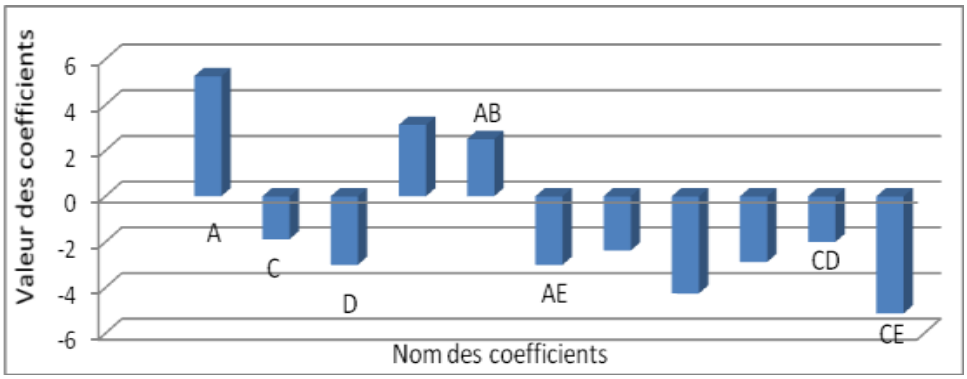

Fig. 3. Bar chart of coefficients

TABLE 5

Coefficient values for the selectivity model

Real Factors	Coded Factors	Estimate of the coefficients	p-value	Signification	Confidence interval at 95%	
					Lowerlimit	Upperlimit
Constant	/	66,44	0,02	Significant	60,09	68,78
Percentage in active phase (%)	A	–3,31	0,11	Not Significant	–7,66	1,03
Temperature (°C)	B	–1,69	0,38	Not Significant	–6,03	2,66
Time (h)	C	–1,69	0,38	Not Significant	–6,03	2,66
Molar ratio	D	11,31	0,01	Significant	6,97	15,66
Catalyst Mass (g)	E	0,56	0,76	Not Significant	–3,78	4,91
	AB	2,56	0,20	Not Significant	–1,78	6,91
	AC	2,81	0,16	Not Significant	–1,53	7,16
	AD	3,31	0,11	Not Significant	–1,03	7,66
	AE	3,81	0,07	Not Significant	–0,53	8,16
	BC	–2,81	0,16	Not Significant	–7,16	1,53
	BD	3,43	0,10	Not Significant	–0,91	7,78
	BE	–3,56	0,09	Not Significant	–7,91	0,78
	CD	0,19	0,93	Not Significant	–5,80	6,17
	CE	–0,56	0,81	Not Significant	–6,55	5,42
	DE	2,19	0,26	Not Significant	–2,16	6,53

$R^2 = 0.92$ and $R^2_{adj} = 0.75$ means that the conversion model is 92% reliable.

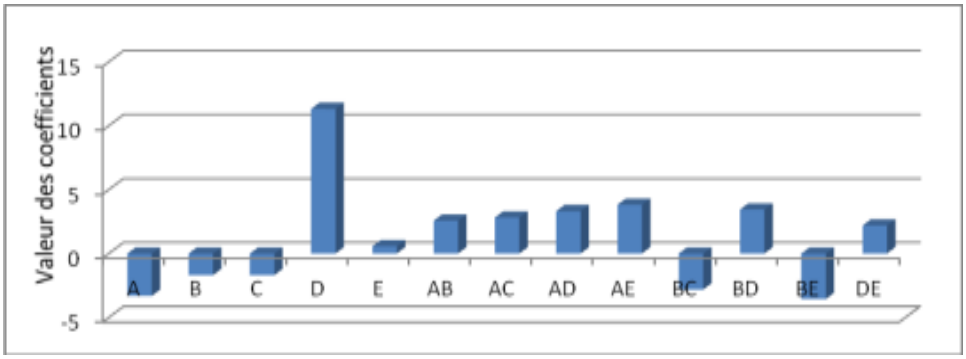

Fig. 4. Bar chart of coefficients

not reach their threshold values to be significant, and the zero belongs to their confidence domains.

D. Optimization

An optimization module was added to the DoE software (Optimization) in order to be able to search for a combination of the factor levels that simultaneously satisfy the goals set for each response. In this study, the desirability function was used to generate parameters of ideal yields. This was achieved by selecting the desired conditions in order to have maximum conversion and selectivity, with equal ranges of importance for all of them. The DoE software generated a list of potential yields, ordering them according to the desirability of the set parameters.

The optimal combination, with parameter values closest to the required values, was found to be the following: catalyst mass = 0.1 g, % active phase = 15%, reaction emperature = 74°C and reaction time = 4 h. (desirability value 1). Under these conditions, the calculated conversion was found to be equal to 49% and the selectivity to epoxide of cyclohexene was equal to 89%.

The maximum values of the response functions, which were calculated using the regression functions, were found to be in good agreement with the experimental values (for the same values of the independent factors), and within the limits of

TABLE 6

Reaction parameters giving optimum responses

Responses	Maximum value		Optimum parameters of the responses				
	Expt.	Calc.	A (%)	B (°C)	C (h)	D	E (g)
Conversion (%)	46	49	+1 (15)	+0,93 (74)	–1 (4)	+1 (1/0,5)	+1 (0,1)
Selectivity (%)	84	89	+1 (15)	+0,93 (74)	–1 (4)	+1 (1/0,5)	+1 (0,1)

experimental errors (TABLE 6). The values of the multidimensional correlation coefficient R. ranged from 0.96 to 0.98 for the response functions under study, confirming that the experimental data are in good agreement with the values calculated from the regression equations.

4. Conclusions

Materials X % V_2O_5/CeO_2 with X = 5, 10 and 15% were prepared by impregnation. According to XRD analysis, the ceria is preserved after impregnation with vanadium, and the results of nitrogen adsorption analysis show an increase in specific surface area due to the dissolution and re-precipitation of ceria during catalyst preparation.

The catalytic activity was evaluated using 3 mL of cyclohexene, 15 mL of heptane, and TBHP as the oxidant under reflux conditions. Several parameters influence cyclohexene conversion and epoxide selectivity, including: percentage of active phase, temperature, time, molar ratio and mass.

To study the influence of each parameter alone, as well as its interaction with another parameter, we have adopted a simple, easy-to-interpret mathematical model: the fractional factorial design 2^{5-1}, analogous to the full factorial design.

Significant parameters influencing conversion are: mass, temperature-molar ratio and time-mass interaction, other parameters have no effect.

Significant parameters influencing selectivity are: molar ratio, other parameters have no effect.

Optimum conditions for the cyclohexene epoxidation reaction are: catalyst mass = 0.1 g, % active phase = 15%, temperature = 74°C and time = 4 h.

These results are valid for a risk threshold of 5% in relation to the model choices and assumptions introduced.

REFERENCES

[1] R.M. Philip, S. Radhika, C.M. Afsina Abdulla, G. Anilkumar, Recent Trends and Prospects in Homogeneous Manganese-Catalysed Epoxidation. Adv. Synth. Catal. **363** (5), 1272-1289 (2021).

[2] J. Liu, R. Meng, J. Li, P. Jian, L. Wang, R. Jian, Achieving high-performance for catalytic epoxidation of styrene with uniform magnetically separable $CoFe_2O_4$ nanoparticles. Appl. Catal. B **254**, 214-222 (2019).

[3] J. Liu, T. Chen, P. Jian, L. Wang, X. Yan, Hollow urchin-like NiO/NiCo2O4 heterostructures as highly efficient catalysts for selective oxidation of styrene. J. Colloid Interface Sci. **526**, 295-301 (2018).

[4] N. Masunga, G.S .Tito, R. Meijboom, Catalytic evaluation of mesoporous metal oxides for liquid phase oxidation of styrene. Appl. Catal. A **552**, 154-167 (2018).

[5] L. Wu, X. Wang, B. Li, Porous core-shell Fe_3O_4@$CuSiO_3$ microsphere as effective catalyst for styrene epoxidation. Colloid Interface Sci. **591**, 153158 (2022).

[6] J. Liu, W. Wang, P. Jian, L. Wang, X. Yan, Promoted selective oxidation of ethylbenzene in liquid phase achieved by hollow $CeVO_4$ microspheres. J. Colloid Interface Sci. **614**, 102-109 (2022).

[7] R. Turco, B. Bonelli, M. Armandi, L. Spiridigliozzi, G. Dell'Agli, F.A. Deorsola, S. Esposito, M. Di Serio, Active and stable ceria-zirconia supported molybdenum oxide catalysts for cyclooctene epoxidation: Effect of the preparation procedure. Catal. Today, **345**, 201-212 (2020).

[8] R. Turco, M. Koliaei, F. Ashouri, S. Mohebbi, A. Wojtczak, A. Kozakiewicz, Oxovanadium(IV) Schiff base complexes derived from 2,2′-dimethylpropandiamine: A homogeneous catalyst for cyclooctene and styrene oxidation. Appl. Catal. A **346**, 65-71 (2008).

[9] S. Goorchibeygi, S. Goorchibeygi, R. Bikas, M. Soleimani, M. Siczek, T. Lis, Molecular structure and catalytic activity of Fe(III) coordination compound with ONO-donor hydrazone ligand in the oxidation of cyclooctene by H_2O_2. J. Mol. Struct. **1250** (1), 131774 (2022)

[10] M. Hasanzadeh Esfahani, M. Behzad, M. Dusek, M. Kucerakova, Synthesis and characterization of a series of acylpyrazolone transition metal complexes: Crystal structures and catalytic performance in the epoxidation of cyclooctene. Inorg. Chim. Acta, **508**, 119637 (2020).

[11] C.A. Wegermann, R.R. Ribeiro, G.M. Ucoski, S. Nakagaki, F.S. Nunes, S.M. Drechsel, Study of the catalytic activity of non-heme manganese complexes toward oxidation of cyclooctene and cyclohexene. Appl. Catal. A **471**, 56-62 (2014).

[12] D. Skoda, K. Kuzelova, R.B. Pricilla, B. Hanulikova, M. Urbanek, A. Styskalik, T. Pokorny, I. Doroshenko, L. Simonikova, I. Kuritka, Microwave-assisted condensation approach for vanadium silicate microspheres and their catalytic activity in cyclohexene epoxidation and ethyl lactate oxidation. J. Ind. Eng. Chem. (2025), In Press. DOI: https://doi.org/10.1016/j.jiec.2025.01.003

[13] S. Hamza. Reguigepose El-Korso, synth and catalytic converter à vanadium base: VO_2-M_xO_y (M = Ti, Si, Al, Zr, Ce). Application to cyclohexene oxidation. PhD thesis. Tlemcen, Algeria (2014).

[14] S. El-Korso, S. Bedrane, A. Choukchou-Braham, R. Bachir, The effect of redox properties of ceria-supported vanadium oxides in liquid phase cyclohexene oxidation. RSC Adv. **5**, 63382-63392 (2015).

[15] B.M. Weckhuysen, D.E. Keller, Chemistry spectroscopy and the role of supported vanadium oxides in heterogeneous catalysis. Catal. Today **78**, 25-46 (2003).

[16] T. Radhika , S. Sugunan, Vanadia supported on ceria: Characterization and activity in liquid-phase oxidation of ethylbenzene, Catal. Comm. 8, 150- 156 (2007).

[17] X. Gao, J-M. Jehng, I. E. Wach, In situ UV–vis–NIR diffuse reflectance and Raman spectroscopic studies of propane oxidation over ZrO_2-supported vanadium oxide catalysts. J. Catal. **209**, 43-50 (2002).

[18] N. Ballarini, F. Cavani, M. Ferrari, R. Catani, U. Cornaro, Oxydehydrogenation of propane catalyzed by V–Si–O cogels: enhancement of the selectivity to propylene by operation under cyclic conditions. J. Catal. **213**, 95-102 (2003).

[19] G.C. Bond, S.F. Tahir, Vanadium oxide monolayer catalysts Preparation, characterization and catalytic activity. Appl. Catal. **71**, 1-31(1991) .

[20] I.E. Wachs, Molecular engineering of supported metal oxide catalysts. Chem. Eng. Sci. (8), 2561-2565 (1990).

[21] H. Zou, M. Li, J. Shen, A. Aroux, Surface acidity of supported vanadia catalysts. J. Therm. Anal. Calorim. **72**, 209-221 (2003).

[22] T. Kataoka, J.A. Dumesic, Acidity of unsupported and silica-supported vanadia , molybdena, and titania as studied by pyridine adsorption. J. Catal. **112** (1), 66-79 (1988).

[23] F. Arena, F. Frusters, A. Parmaliana, Structure and dispersion of supported-vanadia catalysts. Influence of the oxide carrier. Appl. Catal. A **176** (2), 189-199 (1999).

[24] G.T. Went, S.T. Oyama, A.T. Bell, Laser Raman spectroscopy of supported vanadium oxide catalysts. J. Phys. Chem. **94**, 4240-4246 (1990).

[25] A. Khodakov, B. Olthof, A.T. Bell, E. Iglesia, Structure and catalytic properties of supported vanadium oxides: support effects on oxidative dehydrogenation reactions. J. Catal. **181** (2), 205-216 (1999).

[26] S. Bedrane, C. Descorme, D. Duprez, Investigation of the oxygen storage process on ceria-and ceria–zirconia-supported catalysts. Catal. Today **75** (1), 401-405 (2002)

[27] A. Trovarelli, Catalysis by ceria and related materials. Catalytic Science series, vol. 2, Imperial College Press, London, UK, 2002.

[28] M.M. Mohamed, S.M.A. Katib, Structural and catalytic characteristics of MoO_3/CeO_2 catalysts: CO oxidation activity. Appl. Catal. A **287** (2), 236-243 (2005).

[29] S. Bedrane, C. Descorme, D. Duprez, $^{16}O/^{18}O$ isotopic exchange: A powerful tool to investigate oxygen activation on $M/Ce_xZr_{1-x}O_2$ catalysts. Appl. Catal. A **289** (1), 90-96 (2005).

[30] M.A. Bañares, X. Gao, J.L.G. Fierro, I.E. Wachs, Partial oxidation of ethane over monolayers of vanadium oxide. effect of the support and surface coverage. Stud. Surf. Sci. Catal. **110**, 295-304 (1997).

[31] W. Daniell, A. Ponchel, S. Kuba, F. Anderle, T. Weingand, D.H. Gregory, H. Knozinger, Characterization and Catalytic Behavior of VO_x -CeO_2 Catalysts for the Oxidative Dehydrogenation of Propane. Top. Catal. **20**, 65-74 (2002).

[32] M.V. Martínez-Huerta, J.M. Coronado, M. FernándezGarcía, A. Iglesias-Juez, G. Deo, J.L.G. Fierro, M. A. Bañares, Nature of the vanadia–ceria interface in V^{5+}/CeO_2 catalysts and its relevance for the solid-state reaction toward $CeVO_4$ and catalytic properties. J. Catal. **225** (1), 240-248 (2004).

[33] M.A. Bañares, M.V. Martínez-Huerta, X. Gao, I.E. Wachs, J.L.G. Fierro, Identification and roles of the different active sites in supported vanadia catalysts by in situ techniques. Stud. Surf. Sci. Catal. **130**, 3125-3130 (2000).

[34] S. Boudjema, Synthesis of polyoxometalates based on vanadium and/or ruthenium. Application to the epoxidation of cyclohexene. PhD thesis. Tlemcen, Algeria (2015).

[35] J. Matta, D. Courcot, E. Abi-Aad, A. Aboukais, Identification of Vanadium Oxide Species and Trapped Single Electrons in Interaction with the CeVO4 Phase in Vanadium−Cerium Oxide Systems. ^{51}V MAS NMR, EPR, Raman, and Thermal Analysis Studies, Chem. Mater. **14** (10),4118-4125 (2002).

[36] W. Daniell, A. Ponchel, S. Kuba, F. Anderle, T. Weingand, D. Gregory, H. Knözinger, Characterization and Catalytic Behavior of VO_x-CeO_2 Catalysts for the Oxidative Dehydrogenation of Propane. Top. Catal. **20**, 65-74 (2002).

[37] J.H. Kwak, J.E. Herrera, J.Z. Hu, Y. Wang, C.H. Peden, A new class of highly dispersed VO_x catalysts on mesoporous silica: Synthesis, characterization, and catalytic activity in the partial oxidation of ethanol. Appl. Catal. **300** (2) 109-19 (2006).

[38] M. Nandi, A.K. Talukdar, Vanadia loaded hierarchical ZSM-5 zeolite : a promising catalyst for epoxidation of cyclohexene under solvent free condition. J. Porous Mater. **23**, 1143-1154 (2016).

[39] F. Roozeboom, M. Mittelmeijer-Hazeleger, J. Moulijn, J. Medema, V. De Beer, P. Gellings, Vanadium oxide monolayer catalysts. 3. A Raman spectroscopic and temperature-programmed reduction study of monolayer and crystal-type vanadia on various supports. J. Phys. Chem. **84** (21) 2783-2791 (1980).

[40] N. Belaidi, S. Bedrane, A. Choukchou-Braham, R. Bachir, Novel vanadium-chromium-bentonite green catalysts for cyclohexene epoxidation. Appl. Clay Sci. **107**, 14-20 (2015).

[41] X. Gu, J. Ge, H. Zhang, A. Auroux, J. Shen, Structural, redox and acid–base properties of V_2O_5/CeO_2 catalysts. Thermochim. Acta **451** (1-2) 84-93 (2006).

[42] S. Boudjemaa, M. Zerrouki, A. Choukchou-Braham, Optimization and Statistical Modeling of CatalyticCyclohexene Epoxidation with H_2O_2 over Vanadium-Based Polyoxometalates Supported On Montmorillonite as a Green Calalyst. IJSER **7** (11), 2229-5518 (2016).

[43] J. Goupy, L. Creighton, Introduction aux plans d'expérience. 3^{e} ed., 2000 Dunod, Paris.